Time dependent phenomena in transport properties and *I–V* characteristics of a model for driven vortex matter

2004 J. Phys.: Condens. Matter 16 6789

(http://iopscience.iop.org/0953-8984/16/37/015)

INSTITUTE OF PHYSICS PUBLISHING JOURNAL OF PHYSICS: CONDENSED MATTER

J. Phys.: Condens. Matter **16** (2004) 6789–6810 PII: S0953-8984(04)77410-X

Time dependent phenomena in transport properties and I–V characteristics of a model for driven vortex matter

Mario Nicodemi[1,2] **and Henrik Jeldtoft Jensen**[1]

[1] Department of Mathematics, Imperial College, 180 Queen's Gate, London SW7 2BZ, UK
[2] Dipartimento di Scienze Fisiche, Universitá di Napoli 'Federico II', INFM-Coherentia and INFN Via Cintia, 80126 Napoli, Italy

Received 6 March 2004
Published 3 September 2004
Online at stacks.iop.org/JPhysCM/16/6789
doi:10.1088/0953-8984/16/37/015

Abstract

Recent experiments in type II superconductors on the dynamics of vortices driven by external currents have revealed strong off-equilibrium phenomena, such as 'memory' and history dependent effects in I–V characteristics, which set in beyond the regime of validity of current theories on vortex stationary elastic flow. Here we discuss these phenomena in the framework of a simple model of a Monte Carlo interacting lattice gas moving in a pinning background under an external drive. Via computer simulations we give a comprehensive picture of time dependent phenomena in transport properties, response functions and I–V characteristics of the model and outline its quantitative connections to experimental findings.

(Some figures in this article are in colour only in the electronic version)

1. Introduction

I–V characteristics of driven vortex matter in type-II superconductors are an issue of deep theoretical and practical importance [1–4]. Even though their (quasi) stationary elastic regime can be described within collective creep theory [5] or its extensions [1, 6], they exhibit apparent non-elastic behaviours, such as plastic deformations, and strong non-stationary phenomena, such as 'memory effects', found in experiments as well numerical simulations (see [7–14], references therein and below), which are still largely not understood.

In the present paper we discuss these issues in the framework of a schematic model [14] introduced to describe the large scale physics of vortex matter in superconductors, i.e. a driven lattice gas moving, in the presence of thermal agitation, in a disordered pinning background. We show here, via Monte Carlo simulations, that such a schematic model is able to describe many of the above properties of driven vortices, ranging from non-linearities in the I–V characteristic to 'memory' effects, suggesting that it does capture some essential ingredients

of vortex dynamics. The model simplicity makes it understandable in full detail, allowing us to depict a clear picture of its physics. Interestingly, such a model is closely related to a previously introduced driven lattice gas [15] to study off-equilibrium driven systems. These connections can have important consequences for understanding driven vortex matter.

In previous works [14] we have mainly studied the model dynamics in the absence of an external drive, i.e. its magnetic creep, and shown that the model is able to reproduce a broad spectrum of the phenomenology of vortex physics ranging from magnetization loops and their 'anomalous' second peak, logarithmic creep, 'anomalous' finite creep rate for $T \to 0$, 'rejuvenation' and 'hysteresis' of the system response. Here we first depict a clear scenario of many important properties of voltage relaxation and I–V characteristics with their relations to creep phenomena. After that we mainly discuss topics which have raised considerable interest more recently, such as the *peak effect* in the critical current, its relation with phase transitions in the system, or the strong 'ageing' and *memory phenomena* experimentally discovered in the I–V (i.e. history dependent voltage responses or critical current dependences on driving ramp rates). As a result of this study, a comprehensive framework appears of the time dependence discovered in transport properties and their connections to the magnetic phenomena. In a nutshell, under typical conditions, as the voltage is measured, the system exhibits a slow reorganization of its density profile (reorganization is also present in the absence of the drive); this is at the core of the non-linear, non-stationary slow voltage relaxation.

In section 2 we briefly describe the model used here. In section 3 we discuss the properties of voltage relaxation and in section 3.1 its most important characteristic timescale, τ_V. We then discuss the deep relation of τ_V with underlying magnetic relaxation phenomena. Section 3 is concluded by a short summary of its results in section 3.2. In section 4, we investigate I–V characteristics and, in particular, the consequences of the existence of τ_V on their properties and on those of critical currents (such as 'memory effects', see section 4.3). In such a framework we also comment on their off-equilibrium scaling behaviours (see section 4.1) and the presence of a peak effect (PE) in critical currents (see section 4.2). A brief discussion of the effects of pinning properties on the overall scenario is given in section 4.4, and section 4 is concluded by a short summary of its results in section 4.5. Finally, section 5 contains our conclusions.

2. The model

The vortex system in type II superconductors is an excellent laboratory for experimental and theoretical studies of the influence of thermal and quenched disorder on a system of interacting particles. The competition between the random force produced by the static pinning background and an applied force induced by a transport current is studied in a particularly efficient way through the current–voltage (I–V) characteristics (see [1–4] and references therein). The current applied to the superconductor produces a Lorentz's force on the magnetic vortices. If the vortices are free they will move along with the applied force. But vortices in superconductors are basically never free. Bulk and surface pinning together with the interaction amongst the vortices counteracts the applied force. As the applied force becomes sufficiently large to, at least partially, overcome the restrictions from the pinning, the vortices will begin to break loose and move through the superconductor. The onset of motion occurs gradually and this leads to non-linear plastic processes [7, 12, 13]. The consequent voltage drop is a direct measure of the amount of vortex motion. Hence, non-linear I–V characteristics are measured as a result of the complex processes associated with the onset of vortex motion. In the last few years it has also become clear that strong non-stationary phenomena are observed in the vortex system and dynamical effects play an important role in a broad range of temperatures and densities (see [12–14], references

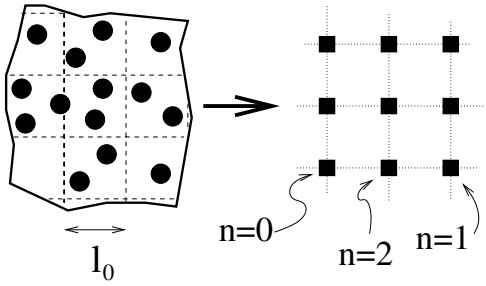

Figure 1. A schematic diagram of the ROM model: the original vortex system (left), described by an off-lattice position field, is coarse grained on a length scale l_0 and mapped into a lattice model, described by a lattice discrete field, where multi-occupancy is allowed (ROM restricted occupancy model).

therein and below). The physics of all these phenomena is the general topic we discuss below.

Since the theoretical investigation of the above complex properties in real systems is hardly achievable in full detail, we consider here a schematic model, called a restricted occupancy model (ROM), described in [14]. We briefly recall its basic features for the sake of clarity.

A system of straight parallel vortex lines, corresponding to a magnetic field B along the z-axis, interacts via a potential [2]: $A(r) = \frac{\phi_0^2}{2\pi\lambda'^2}\left[K_0(r/\lambda') - K_0(r/\xi')\right]$, K_0 being the MacDonald function, ξ and λ the correlation and penetration lengths ($\xi' = c\xi/\sqrt{2}$, $\lambda' = c\lambda$, $c = (1 - B/B_{c2})^{-1/2}$). The typical high vortex densities and long λ imply that the vortex system is strongly interacting. To make it theoretically more tractable, as proposed in [14] (see also [26]), one can coarse grain in the xy-plane by introducing a square grid of lattice spacing, l_0, of the order of the London length, λ (see figure 1). The number of vortices on the ith coarse grained cell, n_i, is an integer number smaller than $N_{c2} = B_{c2}l_0^2/\phi_0$ (B_{c2} is the upper critical field and $\phi_0 = hc/2e$ is the flux quantum). The coarse grained interaction Hamiltonian defining the ROM model is thus [14]: $\mathcal{H} = \frac{1}{2}\sum_{ij} n_i A_{ij} n_j - \frac{1}{2}\sum_i A_{ii}|n_i| - \sum_i A_i^p n_i$. The first two terms describe the repulsion between the vortices and their self-energy, and the last the interaction with a random pinning background. For sake of simplicity, we consider the simplest version of $\mathcal{H}$: we choose $A_{ii} = A_0 = 1$; $A_{ij} = A_1 < A_0$ if i and j are nearest neighbours, $A_{ij} = 0$ otherwise; the random pinning is delta-distributed $P(A^p) = (1 - p)\delta(A^p) + p\delta(A^p - A_0^p)$. Particles are also given a 'charge' $s_i = \pm 1$ (corresponding to opposite direction of magnetic flux) and neighbouring particles with opposite 'charge' annihilate. The values of the model parameters in $\mathcal{H}$ that we use here (exceptions are clearly written) are: $A_1 = 0.28A_0$, $A_0^p = 0.3A_0$, $N_{c2} = 27$, $p = 1/2$. They can be related to the real material parameters as shown in [14].

In analogy with the computer investigation of dynamical processes in fluids [16], the time evolution of the model is simulated by a Monte Carlo Kawasaki dynamics on a square lattice of linear size L at a temperature T. The considered system size is $L = 32$, but our results are checked up to $L = 128$ (and they are robust to changes in $\mathcal{H}$ parameters). The system is periodic in the y-direction. The two edges parallel to the y-axis are in contact with a vortex reservoir, representing an external magnetic field. The reservoir has a particle density N_{ext}. Particles can enter and leave the system only through the reservoir via the same Monte Carlo dynamics above.

The system is prepared by zero field cooling and then increasing N_{ext} at a constant rate up to the working value (usually below $N_{ext} = 10$, a value below the second magnetization

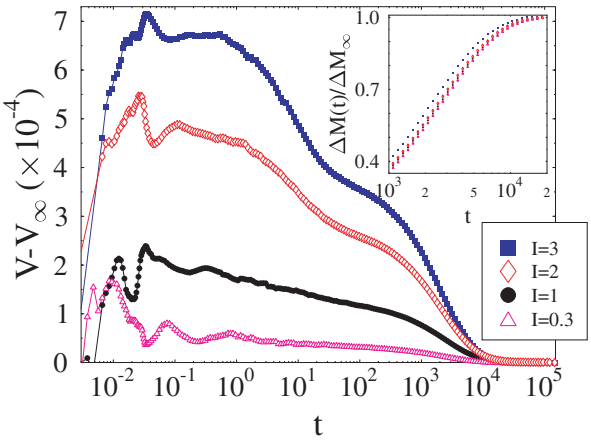

Figure 2. Under a given applied drive I, the voltage, $V(t)$, is recorded as a function of time at $T = 1.0$ ($N_{\rm ext} = 10$). Here we plot $V(t)$ shifted by V_∞ (i.e. its asymptotic value); the four curves correspond to the four shown I. Inset: the decay of the magnetization corresponding to the data of the main panel, shows a very tiny change in the observed range of currents.

peak [14]). For a given applied field, $N_{\rm ext}$, we monitor the system relaxation in the presence of a drive, I, in the y-direction (due to the Lorentz force deriving from a current in the x-direction). As in similar driven lattice gases [15], the effect of the drive is simulated by introducing a bias in the Metropolis coupling of the system to the thermal bath: a particle can jump to a neighbouring site with a probability $\min\{1, \exp[-(\Delta\mathcal{H} - \epsilon I)/T]\}$. Here, $\Delta\mathcal{H}$ is the change in $\mathcal{H}$ after the jump and $\epsilon = \pm 1$ for a particle trying to hop along or opposite to the direction of the drive and $\epsilon = 0$ in orthogonal jumps. A drive I generates a voltage V [30]:0

$$V(t) = \langle v_{\rm a}(t) \rangle \tag{1}$$

where $v_{\rm a}(t) = \frac{1}{2\Delta t} \int_{t-\Delta t}^{t+\Delta t} v(t')\, {\rm d}t'$ is an average vortex 'velocity' in a small interval around the time t. We consider such an average to improve the statistics on $V(t)$ and choose Δt accordingly. Here, t is the Monte Carlo time (measured in units of single attempted update per degree of freedom), $v(t) = \frac{1}{L} \sum_i v_{\rm i}(t)$ is the instantaneous flow 'velocity', $v_{\rm i}(t) = \pm 1$ if the vortex i at time t moves along or opposite to the direction of the drive I and $v_{\rm i} = 0$ otherwise. The data presented below are averaged over up to 3072 realizations of the pinning background (with $A_1 = 0.28A_0$, $p = 0.5$ and $A_0^p = 0.3A_0$, when not otherwise stated) and noise realizations.

3. Voltage time relaxation

The first issue we discuss is the structure of voltage time relaxation. Upon applying a small drive, I, at time $t = 0$, the system response, V, relaxes towards stationarity following an interesting pattern in the time domain. In figure 2 we plot, as an example, the quantity $V(t) - V_\infty$, i.e. the difference in the voltage at time t, $V(t)$, and its I dependent asymptotic limit $V_\infty = \lim_{t\to\infty} V(t)$ as a function of t (for the shown values of I). We plot $V(t) - V_\infty$ instead of just $V(t)$ for the sake of clarity, since $V_\infty(I)$ may change strongly with I (see below). In figure 2 it is apparent that the voltage relaxation, $V(t)$, has two very different parts: at first a rapidly increasing, and very strongly fluctuating, response is seen overshooting the asymptotic value V_∞, later on a very slow decrease towards stationarity follows. For instance, for $I = 3$ in a time interval $\Delta t \simeq 2 \times 10^{-1}$, V leaps from about zero to $\Delta V_{\rm i} \sim 2 \times 10^{-3}$, corresponding

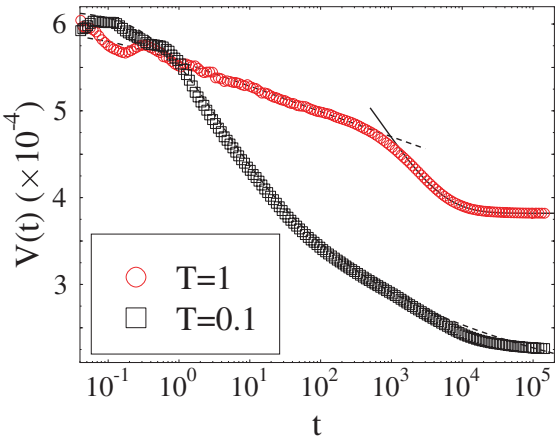

Figure 3. For a given drive $I = 1$, the voltage relaxation, $V(t)$, is plotted as a function of time, t, for the shown values of temperatures ($N_{\rm ext} = 10$). At very low T, the voltage decay with t is approximately logarithmic, while at higher T, an early relaxation (which for small I is approximately logarithmic) is followed by stretched exponentials: $V(t) \propto \exp[-(t/\tau_V)^{\beta_V}]$. The superimposed curves are these fits (see text for details).

to a rate $r_{\rm i} = |\Delta V_{\rm i}/\Delta t| \sim 10^{-2}$. This is to be compared with the rate of the subsequent slow relaxation from, say, $t = 2 \times 10^{-1}$ to $t = 10^4$, $r_{\rm f} \sim 10^{-7}$: $r_{\rm i}$ and $r_{\rm f}$ differ by five orders of magnitude.

The following long time (i.e. $t > 10^0$), slow relaxation of $V(t)$, found for not too low T (see below), has a characteristic double step structure, in agreement with experimental findings [12, 13, 31]. Typically, for not too low temperatures (as shown in figure 3 for $T = 1$), $V(t)$ can be asymptotically well fitted by stretched exponentials:

$$V(t) \simeq V_\infty(I) + \Delta V \exp\left[-\left(\frac{t}{\tau_V}\right)^{\beta_V}\right]. \tag{2}$$

The above long time fit defines the characteristic asymptotic scale, τ_V, of relaxation. The exponent β_V, as well as τ_V, V_∞ and ΔV, are functions of I, T and $N_{\rm ext}$ (see figures 4, 5, 6, 7).

In particular, τ_V drastically increases by decreasing T (see figure 5) and below a crossover temperature $T_{\rm g} \simeq 0.25$ [14], τ_V gets longer than our observation window (and in the meantime β_V becomes much smaller than 1). This corresponds to the fact that below $T_{\rm g}$ on our observation timescales we can no longer approach equilibrium. Actually, below $T_{\rm g}$ a much slower, approximately logarithmic, relaxation is found, as shown in figure 3 for $T = 0.1$: $V(t) \simeq V_\infty + \Delta V[1 + U \ln(\frac{t+t_0}{t_0})]^{-1}$. Interestingly, the same kind of crossover from stretched exponential to logarithms by decreasing T is also observed in magnetic relaxation, as reported in detail in [14], an important fact that we will discuss further later on. In the inset of figure 2, for comparison to $V(t)$ we also plot the relaxation of relative magnetization $\Delta M(t)$ which shows a tiny dependence on I (here $M(t) = N_{\rm in}(t) - N_{\rm ext}$ is the difference of the average vortex density inside, $N_{\rm in}$, and outside, $N_{\rm ext}$, the sample, for more details of the magnetization see [14]).

Figures 2 and 3 also reveal an interesting pre-asymptotic decay of $V(t)$, which shows a pronounced dependence on I: after the first steep rise, for I below a characteristic value $I^* \simeq {\rm O}(1)$, $V(t)$ relaxes approximately logarithmically in t for times up to scales of ${\rm O}(\tau_V)$, while for $I > I^*$ a power law like behaviour precedes the asymptotic stretched exponential of equation (2). This double step structure closely remembers the relaxation of supercooled

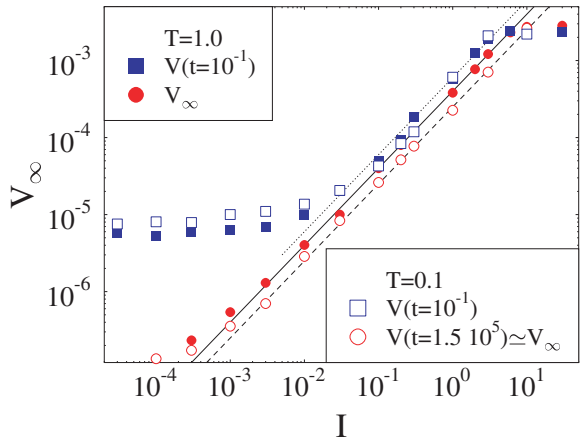

Figure 4. The asymptotic I–V is shown for $T = 1.0$ (filled circles) and $T = 0.1$ (empty circles). It is obtained by applying a drive I and then waiting a very long time to approach the asymptotic stationary value of V. We also show (squares) the I–V obtained by waiting only a 'short' time $t = 10^{-1}$. The differences with the asymptotic I–V are apparent.

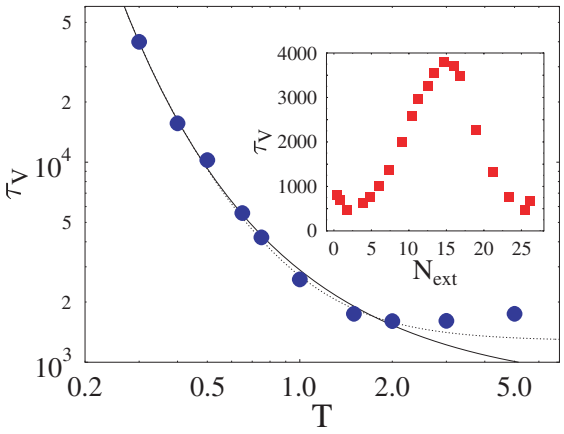

Figure 5. The characteristic timescale of voltage relaxation, $\tau_V(T)$, as a function of T (for $I = 1$ at $N_{\rm ext} = 10$). The superimposed curves are the fits discussed in the text. Inset: τ_V is non-monotonous as a function of $N_{\rm ext}$ with a maximum corresponding to the location of the second magnetization peak (here $I = 1$ at $T = 1$).

liquids described by mode coupling theory [23]. Actually, we have already discussed the relations between the present model for vortex matter and fragile glass formers in [14] which we refer to for further detail.

The above results clearly point out that since V is a function of time (at least for $t \leqslant \tau_V$), the I–V itself can be strongly time dependent whenever the system is probed or driven on timescales shorter than τ_V. In figure 4 we plot the *asymptotic* I–V, i.e. the function $V_\infty(I)$ (for $N_{\rm ext} = 10$): V_∞ appears to be linear on I in several orders of magnitude in the whole range of temperatures we considered, $T \in [0.1, 5]$. Notice that, due to the intrinsic lattice nature of our model, for $I \to \infty$ $V_\infty(I)$ tends to saturate to a finite plateau. In figure 4 we also show the voltage corresponding to time $t = 10^{-1}$, $V(t = 10^{-1})$, as a function of I; this outlines the difference with $V_\infty(I)$. Later on we will discuss in deeper detail the I–V characteristic

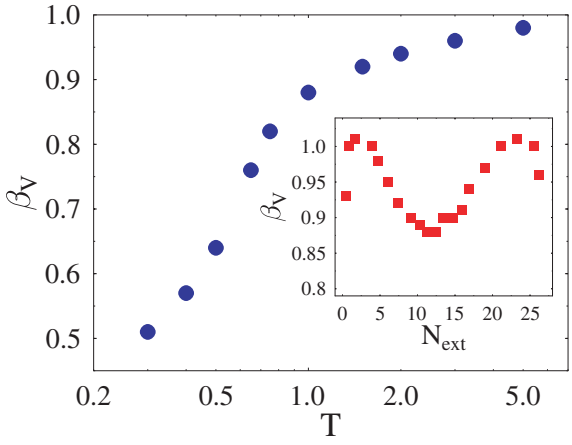

Figure 6. The exponent of the stretched exponential relaxation, $\beta_V(T)$, as a function of T (for $I = 1$ at $N_{\rm ext} = 10$): β_V decreases from about 1 (corresponding to standard exponential relaxation) at high T to comparatively smaller values at low T. Inset: β_V is plotted as a function of $N_{\rm ext}$ ($I = 1$ at $T = 1$).

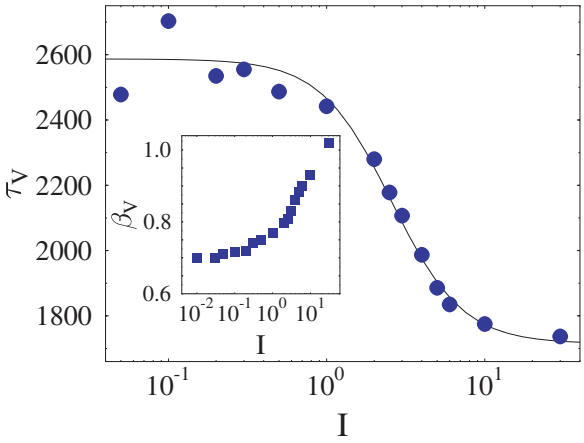

Figure 7. The characteristic timescale of relaxation, $\tau_V(I)$, as a function of the applied drive I. For $I \to 0$, $\tau_V(I)$ saturates to a *finite* value which implies that the asymptotic critical current is $I_{\rm c} = 0$. Inset: β_V is plotted as a function of I ($T = 1$, $N_{\rm ext} = 10$).

recorded when the system is far from stationarity, as for instance when at low temperatures τ_V is large enough for the asymptotic behaviour being unreachable on finite observation time scales.

3.1. Equilibration time

One of the most important physical quantities individuated by the above analysis of the voltage relaxation, is the system characteristic timescale τ_V. It is the determinant for understanding the system dynamics and its approach to equilibrium (see [14]). Let us consider first the temperature dependence of τ_V, shown in figure 5. In our model, in the region where τ has a steep increase with T a Vogel–Tamman–Fulcher (VTF) law fits the data (see the continuous

curve in figure 5):

$$\tau_V(T) = \tau_0 \exp\left[\frac{E_0}{(T - T_c)^\nu}\right] \tag{3}$$

with $\tau_0 \simeq 7 \times 10^2$, $\nu \simeq 0.9$ and $T_c \simeq 0.01$. The best value fit for T_c is then a number numerically indistinguishable from zero. This fact confirms that in the present 2D version of the model the glass transition is pushed at $T = 0$ [14].

We notice that in the low T regime a power law divergence also fits the data, as shown by the dotted curve of figure 5: $\tau_V = \tau_0 (T - T_c)^{-\nu} + \tau_\infty$, with $\tau_0 \simeq 1.1 \times 10^3$, $\tau_\infty \simeq 1.3 \times 10^3$, the exponent $\nu \simeq 2$ and $T_c \simeq 0.1$. The presence of a strong increase of τ close to a VTF law (or an Arrhenius since $T_c \sim 0$) or a power law is again a mark of the apparent similitude with glassy features of supercooled liquids and glasses [23, 24, 28, 29]. We stress that, in this scenario, T_c represents the location of an 'ideal' transition, as T_g (defined above) is just a crossover point where relaxation timescales of the dynamics get longer that our observation window (here about 10^5).

In the inset of figure 5, we show for completeness the dependence of τ_V on N_{ext}. Interestingly, τ_V is non-monotonous with N_{ext} showing an apparent maximum around the value corresponding to the second peak in magnetization loops $N_{ext} \sim 13.5$ [14]. The increase in $\tau_V(N_{ext})$ found at very small or large N_{ext} are associated to the small and large field first order melting transitions [14], where the system has a transition from a disordered state to an ordered one. In figure 6 we show the values of the exponent β_V corresponding to the τ_V of figure 5 (the data in figures 5 and 6 are for $I = 1$). The figure shows that β_V decreases from a value of about 1 (corresponding to a simple exponential) at high T to about 0.5 for $T = 0.3$. This is again a behaviour very close to the one found in other glassy systems. The non-monotonous behaviour of $\tau_V(N_{ext})$ is found in a similar way in $\beta_V(N_{ext})$ (see inset of figure 6).

Very important is the behaviour of τ_V on changing the driving I, shown in figure 7 for $T = 1$ and $N_{ext} = 10$: $\tau_V(I)$ increases by decreasing I and seems to approach a *finite plateau* for $I < I^*$, with $I^* \simeq O(1)$. The higher the drive I the faster the approach to stationarity and, in this sense, an increase in I has an effect similar to an increase in T. Notice that such a result is in agreement with experimental findings [12] and with analogous features observed in other driven lattice gases [15]. The superimposed curve in figure 7 is a power law fit:

$$\tau_V(I) = \frac{\tau_V^0 - \tau_V^\infty}{[1 + (I/3I^*)^y]} + \tau_V^\infty \tag{4}$$

where, for $T = 1$, $N_{ext} = 10$ and $A_p = 0.3$ we find with $\tau_V^0 = 2.6 \times 10^3$, $\tau_V^\infty = 1.7 \times 10^3$, $I^* = 0.9$ and the new exponent $y \simeq 2$. Finally, in an inset of figure 7 we also show the function $\beta_V(I)$. Experimentally, the existence of a characteristic time decreasing with I approximately as a power law has been reported in the third reference of [12], also the exponent y from experimental data is larger than ours reported above.

Let us notice that the existence at $T = 1$ of a *finite* τ_V limit for $I \to 0$ implies that the flux flow can be activated for any finite I. This confirms that the system's asymptotic (i.e. for $t \to \infty$) critical current, I_c, is zero for[3] $T = 1$. The asymptotic value of I_c can be expected to be non-zero at lower T or for stronger pinning, as shown later on. The above reasoning for instance may suggest that in the region $T < T_c$, since $\tau_V(I) \to \infty$ for $I \to 0$, a true asymptotic finite I_c can be found, T_c being the *ideal glass transition* point [1, 14], where by definition $\tau_V(T)|_{I=0}$ diverges. A consequence of the existence of a finite I_c for $T < T_c$ would

[3] The reasoning can be briefly restated as follows: if I_c is non-zero then, at least for I small enough, vortices cannot diffuse; thus they must be 'frozen' and τ_v be very large (infinite).

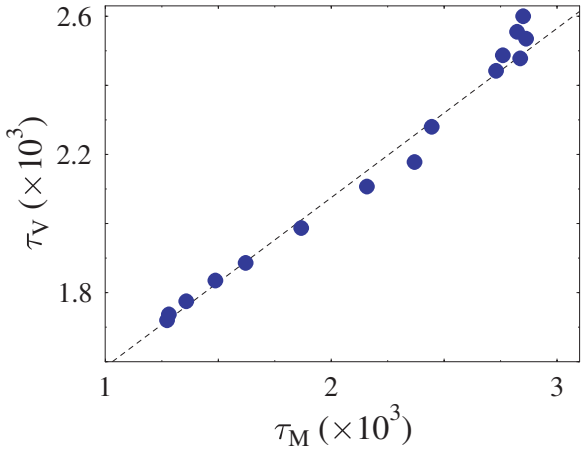

Figure 8. Vortex driven flow and creep are closely related. Actually, the characteristic timescales of voltage relaxation, $\tau_V(I)$, and of magnetic creep, $\tau_M(I)$, are approximately proportional (here shown for $T = 1$ and $N_{ext} = 10$).

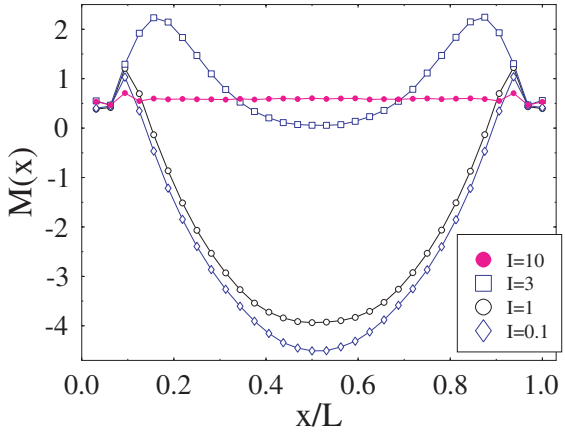

Figure 9. The Bean magnetization profile, M, present in the system after a given time $t = 10^5$ is plotted as a function of the coordinate x in the system ($x \in [0, L]$) orthogonal to the direction of the drive, for the shown values of the applied drive I ($T = 0.1$, $N_{ext} = 10$).

be the possibility of vortex flow without dissipation first discussed by Fisher [1]. In the present context such a scenario is consistent, but cannot be tested because of the above discussed huge relaxation time found at low T and a T_c numerically indistinguishable from zero.

The time dependent properties of the driven flow, and in turn those of I–Vs, are strongly linked to the concurrent vortex creep and reorganization of vortex domains. In fact, both with or without an external drive, the system evolves in the presence of a Bean-like profile [32] (see figure 9) which also relaxes with a characteristic timescale τ_M [14]. This phenomenon, in the absence of an external drive, has been experimentally observed in detail for instance in [33]. An important discovery is that $\tau_M(I)$ and $\tau_V(I)$ are approximately proportional, as shown in figure 8. This outlines that the strong non-linear, non-stationary voltage relaxation is structurally related to the reorganization of vortices during the creep (a fact in agreement with recent experiments [22]). In particular, in figure 9 we show the magnetic spatial profile

present in the system (at $T = 0.1$ and $N_{\rm ext} = 10$) after a drive I has been applied for a given time $t = 10^5$: consistent with the above scenario, the larger I is, the flatter the Bean profile, which corresponds to shorter τ_V.

3.2. Summary

Summarizing, in this section we have investigated, in full detail, the properties of voltage relaxation in the ROM model at given values of the control parameters, T, $N_{\rm ext}$ and I. The function $V(t)$ has *two different parts* with very different behaviours: at first a rapidly increasing, and very strongly fluctuating, response is seen overshooting the asymptotic value V_∞, later a slow decrease towards stationarity follows. The latter, in its long time behaviour, is an approximately *stretched exponential* and, for very low T, *logarithmic*. The relevant quantity governing the long time decay is the *equilibration time*, $\tau_V(T, N_{\rm ext}, I)$, needed for vortex relaxation towards equilibrium. The important emerging features are that τ_V appears to *exponentially diverge* as $T \to 0$ and it is a *non-monotonous* function of the applied field, $N_{\rm ext}$, with a well defined maximum around the second magnetization peak location, corresponding to the peak position in the peak effect observed in critical currents (see below). Importantly, τ_V depends on the drive I, decreasing approximately as a *Lorentzian* when $I \to \infty$. An important discovery is that voltage and magnetic relaxations are strongly linked: in brief, while the voltage is being measured, the system Bean profile (i.e. density profile) typically undergoes a slow (usually almost logarithmic) reorganization (which is also present in the absence of the drive); this induces, in turn, the non-linear shapes of I–V and the non-stationary slow voltage relaxation.

4. I–V characteristics

In the above section we have outlined the existence of characteristic timescales, in particular $\tau_V(I, T, N_{\rm ext})$, which play an important role in the process of voltage relaxation of the driven system. We are going to consider now some more general features of I–V characteristics and, in particular, the effects of the presence of a finite τ_V, which cannot be ignored above all at low T. For instance, whenever the system is perturbed and observed on timescales shorter than the time needed to approach stationarity, τ_V, strong 'hysteresis' and 'memory' phenomena are going to appear.

In the present model the I–V characteristics are recorded as in real experiments: after fixing the working conditions (i.e. temperature, T, and external field, $N_{\rm ext}$), the function $V(I)$ is recorded by ramping up the drive I from zero at a given rate $\gamma_I = {\rm d}I/{\rm d}t$ and by collecting the corresponding values of V. We notice immediately that in all the situations when $\gamma_I > \tau_V^{-1}$ the function $V(I)$ will depend on the system history, simply because the system has not been able to follow the applied drive. In fact, it is now experimentally well established that I–V characteristics can show strong 'memory' phenomena in typical working situations (see for instance [12, 13, 20] and references therein).

As an example of the I–V found in the present model, in figure 10, we plot the I–V recorded after ramping I (with a rate $\gamma_I = 5 \times 10^{-3}$) at $T = 1$ (filled squares) and at $T = 0.1$ (open circles) for an applied field of $N_{\rm ext} = 10$. The low T I–V appears to have the typical S shaped form experimentally found [3, 4, 12, 13, 18, 19]. As a matter of fact, the I–V are dependent on the ramp rate γ_I (see figure 12) and their S shape tends to disappear when $\gamma_I \to 0$: the S shape in the I–V of the present model is an effect of short times of relaxation allowed in the system by the comparatively too large γ_I. The continuous ($T = 1$) and dotted ($T = 0.1$) lines in figure 10 are, in fact, the *asymptotic* I–V, $V_\infty(I)$ we discussed in the

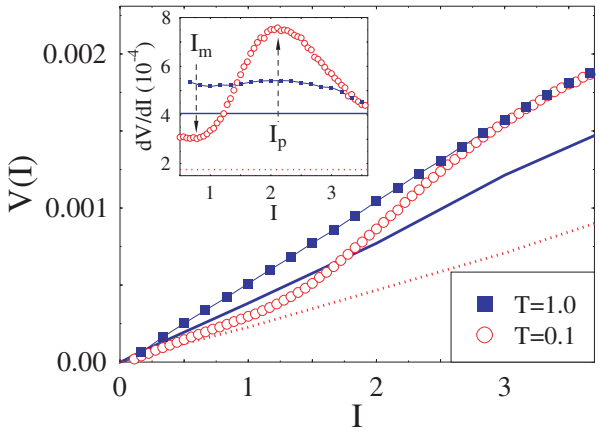

Figure 10. The I–V is recorded by ramping I with a rate $\gamma_I = \mathrm{d}I/\mathrm{d}t = 5 \times 10^{-3}$ for the shown T, at $N_{\mathrm{ext}} = 10$. The continuous and dotted curves (respectively $T = 1, 0.1$) are the *asymptotic* I–V, i.e. those where, for a given I, V is measured after waiting $t = 10^5$ (see figure 2). Inset: the differential resistivity, $\rho = \mathrm{d}V/\mathrm{d}I$, for the same data of the main panel. The horizontal lines are from a linear fit to the *asymptotic* I–V. The characteristic values I_m and I_p roughly locate crossover points in the 'short time' ρ, which, however, disappear if $t \to \infty$. (Figure from [14].)

previous section, i.e. those recorded after applying a drive I and measuring V after waiting a time long enough (here $t = 1.5 \times 10^5$). As stated, for finite γ_I, the I–V is non-Ohmic with a power law behaviour at low I [39]: $V \simeq \rho_0 I^{\alpha}$ where the exponent α, in general, is field and temperature dependent (see [39]). For instance, α is about 1.3 for $\gamma_I = 5 \times 10^{-3}$, $N_{\mathrm{ext}} = 10$ and $T = 0.1$ (see below). At larger values of I an Ohmic behaviour is observed [39].

Of practical relevance is one of the observable effects found for large rates γ_I: the effective resistivity measured in the sample is *larger* than the intrinsic one (i.e. the one relative to the 'asymptotic I–V'). This is clearly shown by the differential resistivity, $\rho = \mathrm{d}V/\mathrm{d}I$, plotted in the inset of figure 10, where again the horizontal continuous and dotted lines correspond to the asymptotic Ohmic behaviour.

The non-monotonous behaviour of the finite γ_I differential resistivity, $\rho(I)$, has often been interpreted as a signal of the presence of different regimes in the vortex flow, separated, for instance, by the location of the thresholds I_m and I_p shown in the inset of figure 10. In the present context, however, it appears that they are just transient effects in the non-stationary regime observed for comparatively too fast γ_I. The linear behaviour of the asymptotic I–V indeed shows that these 'crossovers' in the 'short time' $\rho(I)$ tend to slowly disappear with time, thus they cannot correspond to transitions among different driven stationary phases [7, 8, 10–13, 35]. This conclusion holds despite the regular behaviour of I_m and I_p with T also experimentally seen (for instance, I_p seems to grow with T). An intrinsic structure in the function $\rho(I)$ can possibly be observed at sufficiently lower currents and temperatures [35]. Interestingly, at $T = 0$ crossovers between different plastic channels flow regimes are indeed typically found in the present model as well as in more realistic models (see discussions in [7, 8, 26, 27, 35] and references therein). For instance, in [26] (where, actually, a different definition of V and I is used) the flow at $T = 0$ in the region $I < I_m$ was shown to be characterized by 'filamentary channels', around I_p by 'braided rivers' and only at higher I it becomes a 'full flow'. Thus, here at $T = 0.1$ the thresholds I_m and I_p might be the off-stationarity, finite temperature rests of these transitions in the nature of vortex flow properly defined only at $T = 0$.

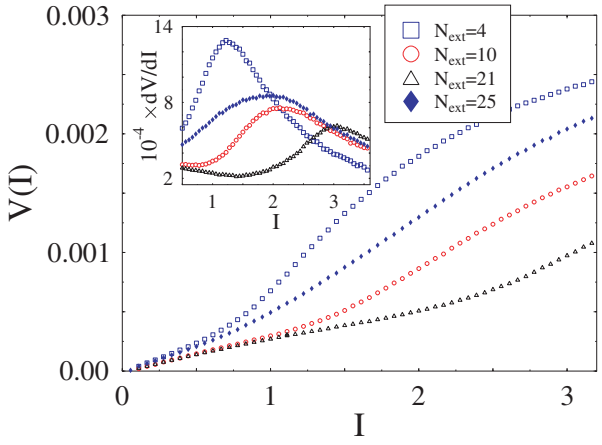

Figure 11. As in figure 10 the I–V is recorded by ramping I with rate $\gamma_I = \mathrm{d}I/\mathrm{d}t = 5 \times 10^{-3}$ at $T = 0.1$ for the shown N_{ext}. Inset: the differential resistivity, $\rho = \mathrm{d}V/\mathrm{d}I$, for the same data of the main panel.

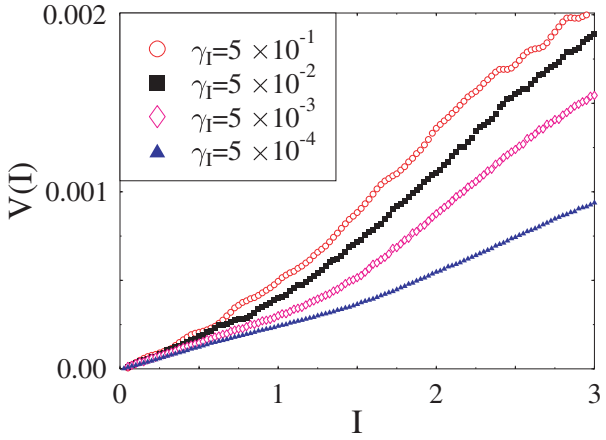

Figure 12. At low temperatures the dependence of the I–V on the driving ramp rate γ_I becomes apparent. The four curves plotted here are data collected at the same temperature and external field ($T = 0.1$, $N_{\mathrm{ext}} = 10$), but correspond to the different shown values of $\gamma_I = \mathrm{d}I/\mathrm{d}t$.

For sake of completeness, we show in figure 11 the appearance of the I–V characteristics, $V(I)$, and differential resistivity, $\rho(I)$, for $T = 0.1$ recorded for several applied fields taken from a broad range of values. Notice the non-monotonous behaviour of I_p with N_{ext}. Finally, in figure 12 for a system at $T = 0.1$ and $N_{\mathrm{ext}} = 10$, we show the effects on the I–V of different current ramping rates $\gamma_I = \mathrm{d}I/\mathrm{d}t$. In particular, it is apparent that by lowering γ_I the resistivity decreases, a fact in correspondence with experimental findings [13].

4.1. Off-equilibrium scaling of I–V at small I and T

Now we consider in some details the temperature dependence of the I–V. In figure 13 we show the isothermal functions $V(I)$ recorded, with a ramp rate $\gamma_I = 5 \times 10^{-4}$, at several

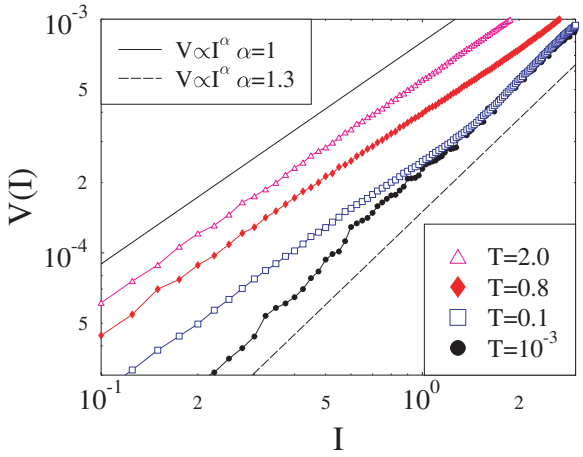

Figure 13. We plot the small currents region of the I–V, recorded at the shown temperatures, in a log–log plot (here $N_{\rm ext} = 10$, $\gamma_I = 5 \times 10^{-4}$). At high T the I–V is Ohmic, but by lowering T an apparent departure from linearity is observed, with a new non-trivial long power law region emerging at low I. Notice that the data at low temperature are taken while the system is very far from equilibrium.

temperatures in the presence of an applied field $N_{\rm ext} = 10$. By decreasing T, the I–V curves become less and less Ohmic and, at very low T, they tend to collapse one on top of the others on a sort of 'limit function' close to a non-trivial power law (the dashed line in figure 13): $V \sim I^{\alpha}$ with $\alpha \sim 1.3$ for $T \to 0$.

The structure of the isothermal I–V appears to be qualitatively very close to the one experimentally found (see [4, 18–21, 36, 37] and references therein). Interestingly, despite the fact that at low T the system is far from stationarity, in such a region the I–V can be approximately rescaled using the scaling relation originally proposed by Fisher [36] and believed to signal the presence of a 'vortex glass' transition in vortex matter [36, 37]:

$$\frac{V}{I|T - T_{\rm c}|^{\nu(z+2-d)}} = F\left(\frac{I}{|T - T_{\rm c}|^{\nu(d-1)}}\right). \tag{5}$$

From equation (5), as proposed in [36], we define $I' = I/|T - T_{\rm c}|^{\nu(d-1)}$ and $V' = V/|T - T_{\rm c}|^{\nu(z+1)}$, and plot in figure 14 the quantity $\ln(V'/I')$ as a function of $\ln(I')$. In figure 14 we have only included data for $T \leqslant 0.1$, cut off the high I region where the I–V saturate and averaged the data in bins in order to avoid having too noisy points with a plot drastically worsened. The quality of the obtained scaling is certainly not excellent, but two distinct regions definitely seem to appear: a flat low I part followed by a power law low at higher I. Approximate I–V scaling plots, with the same structure of figure 14, have been experimentally found in systems where $T_{\rm c}$ is zero [34]. The scaling exponents used in figure 14 are $\nu \sim 0.35$, $z \sim 1.6$, while $T_{\rm c} \sim 10^{-4}$ is consistent with zero and with our previous results on the behaviour of the $T = 0$ divergence of τ_V. The present values of the critical exponents differ from those experimentally found, the model being too schematic, but are surprisingly close to those found in a much more realistic XY model with random pinning [38].

Importantly, the present discovery of an approximate scaling structure for I–V recorded far from stationarity is experimentally confirmed by very recent observations [20]. However, it is not clear whether the above approximate scaling is either just an artifact resulting from not clean enough data, or an interesting manifestation of equilibrium critical scaling in off-

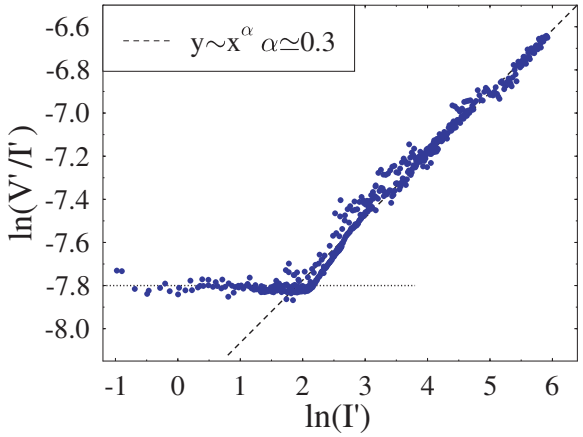

Figure 14. The I–V data at low T from figure 13 are rescaled using the scaling functions proposed by Fisher (see text). Although the quality of the scaling is to some extent poor, a rough structure seems to emerge with a constant part followed by a power law. We have only considered data for $T \leqslant 0.1$ (more precisely, $T = 10^{-3}, 5\times10^{-3}, 10^{-2}, 5\times10^{-2}, 10^{-1}$), else the scaling drastically worsens. We have also cut off the region where the I–V saturate. The scaling parameters are: $\nu \simeq 0.35$, $z \simeq 1.6$ and $T_c \simeq 10^{-4}$.

equilibrium off-stationarity states, or whether it really corresponds to a new form of scaling appearing in the far from equilibrium dynamics.

4.2. Critical currents and resistivities

From the I–V characteristic it is possible to extract information of practical relevance such as critical currents and resistivities. This we now analyse in some detail, focusing in particular on their dependences on temperature, T, applied field, $N_{\rm ext}$, and current ramp rate, γ_I. As in experiments, we define the *'effective'* critical current, $I_c^{\rm eff}$, by a so-called 'voltage criterion': $I_c^{\rm eff}$ is the current value where V gets larger than $V_{\rm thr} = 5\times10^{-5}$. We call $I_c^{\rm eff}$ an 'effective' critical current since we show below that generally it does not represent an 'intrinsic' material parameter. In fact, defined in this way, the critical current is a quantity which, for a given T and $N_{\rm ext}$, may depend on the sample history and on γ_I as well (see figure 15). A better definition for an *intrinsic* critical current, I_c, comes from the asymptotic I–V, $V_\infty(I)$, that we introduced and discussed above in the present paper; actually, $V_\infty(I)$, is by definition not 'history' dependent. $I_c^{\rm eff}$ is a more practical quantity, since it can be easily obtained, and it coincides with I_c whenever the system is probed on timescales longer than τ_V (typically, this is not the case in the system 'glassy' region).

Our data about the effective critical current are shown in figure 15. In the left panel of figure 15 we plot the dependence of $I_c^{\rm eff}$ on the temperature (for $N_{\rm ext} = 10$ and $\gamma_I = 5\times10^{-4}$). We find that at low T $I_c^{\rm eff}$ decays approximately as a power law with T:

$$I_c^{\rm eff}(T) \simeq \frac{I_0}{(1+\frac{T}{T_0})^{x_T}} \tag{6}$$

where $I_0 \simeq 0.3$, $T_0 \simeq 0.6$ and the exponent $x_T \simeq 0.4$ (the continuous curve in the left panel of figure 15). The above fit is reasonable in the low T region (over several decades), but above $T \sim 1$ a drastic change is observable: an *increase* of $I_c^{\rm eff}$ with T, analogous to the one experimentally found, called the peak effect (PE). The PE, i.e. a sharp peak observed

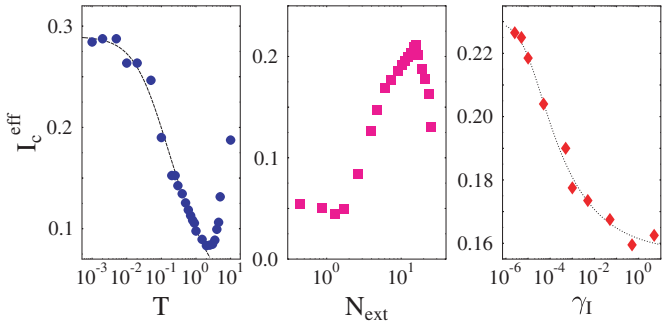

Figure 15. The critical current $I_c^{\rm eff}$ is plotted as a function of T (left panel, where $N_{\rm ext} = 10$ and $\gamma_I = 5 \times 10^{-4}$), $N_{\rm ext}$ (central panel, where $T = 0.1$ and $\gamma_I = 5 \times 10^{-4}$) and $\gamma_I = {\rm d}I/{\rm d}t$ (right panel, where $T = 0.1$ and $N_{\rm ext} = 10$). $I_c^{\rm eff}$ is defined as the point where $V = 5 \times 10^{-5}$. The superimposed curves are the fits discussed in the text. Interestingly, the so-called *peak effect* is clearly observable. In particular, the peak in $I_c^{\rm eff}$ as a function of $N_{\rm ext}$ in the present model corresponds to the second magnetization peak found in hysteretic loops. The sudden rise in $I_c^{\rm eff}$ as a function of T is related to the melting transition. Also notice the non-equilibrium effects observed at low T, as shown by the γ_I dependence plotted in the right panel.

in the critical current (or a deep in resistivity) when plotted, for instance, as a function of the applied field or temperature [22, 40–43], is a ubiquitous phenomenon observed in vortex physics of type-II superconductors. In recent years important theoretical [44–46] and experimental [33, 41–43, 47] aspects of the PE have been clarified, showing, in particular, that the PE is associated to new phase transitions occurring in the system. However, important questions are still open, as those concerning the origin of the strong dynamical anomalies discovered in the PE region, including 'memory' effects, 'history' dependence and apparent metastability phenomena [12, 17, 41, 43, 48]. This can be clarified by considering the structure of τ_V, as already discussed in [14, 39], and explained in full detail below.

Actually, in the present framework, the PE is even more apparent when $I_c^{\rm eff}$ is plotted as a function of $N_{\rm ext}$, as shown in the central panel of figure 15 for $T = 0.1$. Our data closely resemble those experimentally found [41, 49]. The location of the maximum in the PE, $N_{\rm PE}$, is dependent on the ramping rate γ_I as discussed below, but importantly it is very close to the values of the *second magnetization peak* found in magnetic loops, $N_{\rm sp}$ [14, 39]; $N_{\rm PE}$ for $\gamma_I \to 0$ is numerically equal to the equilibrium value of $N_{\rm sp}$. In brief, in the present model the PE is the manifestation in the *driven* system of a first order phase transition found at *equilibrium* in the absence of drive and associated to a 'second peak' in magnetization measures [39]. Finally, in the right panel of figure 15 we show that, at low T, the value of the critical current is definitely dependent on the current ramp rate γ_I. In particular, at $T = 0.1$ and $N_{\rm ext} = 10$ we found [39] that $I_c^{\rm eff}$ decreases by increasing γ_I approximately according a power law (the dotted curve in the right panel of figure 15):

$$I_c^{\rm eff}(\gamma_I) \simeq \frac{I_0}{(1 + \frac{\gamma_I}{\gamma_I^0})^{\Delta_I}} \tag{7}$$

where $I_0 \simeq 0.7$, $\gamma_I^0 \simeq 10^{-5}$ and the exponent $\Delta_I \simeq 0.2$.

Along with $I_c^{\rm eff}$, we report on the properties of the resistivity, $R = V/I$ (which by definition of $I_c^{\rm eff}$ is strictly related to it), and the differential resistivity, $\rho = {\rm d}V/{\rm d}I$. We have already discussed in the previous sections the I dependence of R and ρ, thus below we only consider R and ρ data obtained by an average in the current interval $I \in [0.1, 0.5]$ (which is located in the small current region of the I–V, see figures 10–13). Such an average allows us to simplify the discussion and to show cleaner data.

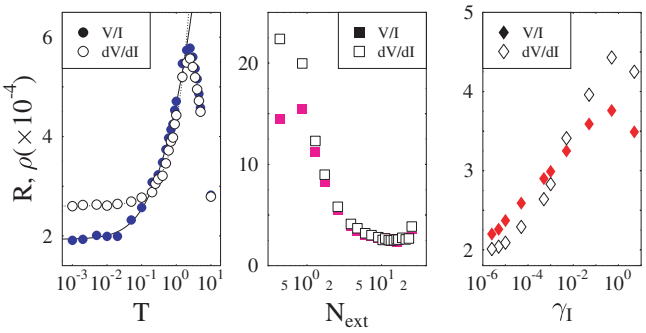

Figure 16. The averaged resistivity, $R = V/I$ (filled symbols), and differential resistivity, $\rho = \mathrm{d}V/\mathrm{d}I$ (empty symbols), defined in the text are plotted as a function of T (left panel, where $N_{\mathrm{ext}} = 10$ and $\gamma_I = 5 \times 10^{-4}$), N_{ext} (central panel, where $T = 0.1$ and $\gamma_I = 5 \times 10^{-4}$) and γ_I (right panel, where $T = 0.1$ and $N_{\mathrm{ext}} = 10$). The superimposed curves are the fit discussed in the text. In particular, notice the saturation towards a finite value of R and ρ at very low T. This phenomenon is analogous for transport properties to the existence of a finite magnetization creep rate found at vanishingly small T. It is an *off-equilibrium* effect.

Of particular interest is the dependence of R and ρ on the temperature T (left panel figure 16). In fact, one observes that, at very low T, R and ρ seem to saturate to a *finite* value. In particular, at low T, the following fits are reasonable (respectively the continuous and dotted curves in the left panel of figure 16):

$$R(T) \simeq R_0 \left(1 + \frac{T}{T_R}\right)^s; \qquad \rho(T) \simeq \rho_0 \left(1 + \frac{T}{T_\rho}\right)^{s'} \tag{8}$$

where $R_0 \simeq 2 \times 10^{-4}$, $T_R \simeq 0.1$, $s \simeq 0.3$, and $\rho_0 \simeq 2.6 \times 10^{-4}$, $T_\rho \simeq 1.5$, $s' \simeq 1.0$. The above finite resistivity values for $T \to 0$ are closely related to the saturation of the magnetic creep rate, $S(T)$, found in the present model [14]. We notice that the value of the exponent $s \sim 0.3$ is very close to the one independently calculated by the I–V scaling $\Delta R(T) \sim |T - T_{\mathrm{c}}|^{\nu(z-d+2)}$ with $\nu(z - d + 2) \sim 0.2$ as predicted in [36].

Notice that in the present schematic lattice model an interesting counterintuitive effect is observed: R and ρ, at higher T, start decreasing with the temperature. This is a non-obvious fact, which is the analogue of the peak effect in $I_{\mathrm{c}}^{\mathrm{eff}}$ reported above. The origin of this phenomenon is related to the presence of a phase transition in the lattice system corresponding with the peak in R of figure 16. This finding is in agreement with the interpretation proposed in [50], but the actual mechanism underlying such an effect in our model is different from the one of [50]. Finally, in the central and left panel of figure 16 we show the behaviours of R and ρ with N_{ext} and γ_I.

4.3. Memory phenomena in I–V characteristics

Another effect of the existence of a long, even though finite, equilibration timescale, τ_V, in the system is the presence at low T of strongly 'history' dependent properties of the current–voltage characteristic. We have already discussed this issue in [14] and here, for sake of completeness, we just connect it to the general features of voltage relaxation we have considered above.

At a given value of T and N_{ext}, as in real experiments on vortex matter [13], we let the system undergo a current step of height I_0 for a time t_0 before starting recording the I–V by ramping I, as sketched in the inset of figure 17. Figure 17 shows (for $T = 0.1$, $N_{\mathrm{ext}} = 10$) that the I–V depends on the waiting time t_0. The system response is 'ageing': the longer t_0

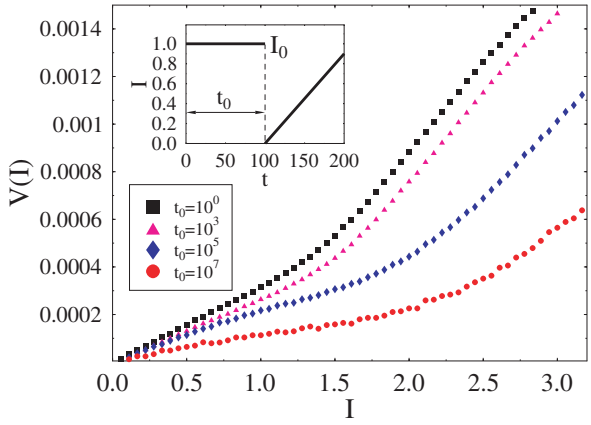

Figure 17. The I–V, at $T = 0.1$ with $N_{\rm ext} = 10$, obtained by ramping I after keeping the system in the presence of a drive $I_0 = 1$ for a time t_0 as shown in the inset. The response, V, is 'ageing' (i.e. depends on t_0) and, more specifically, *stiffening*: it is smaller the longer t_0. (Figure from [14].)

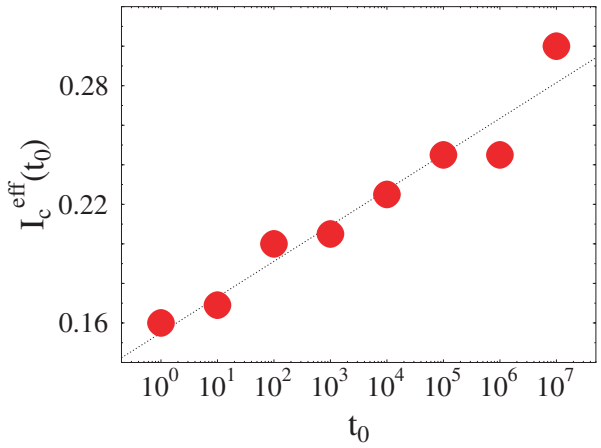

Figure 18. From the data of figure 17, we can define the critical current, $I_{\rm c}^{\rm eff}$, as the point where $V = 5 \times 10^{-5}$. Interestingly, in agreement with recent experimental data, $I_{\rm c}^{\rm eff}(t_0)$ is logarithmically increasing with the time, t_0, the system spent under the current step. The superimposed curve is the fit discussed in the text.

the smaller the response, a phenomenon known as *'stiffening'* in glass formers [24, 25]. These effects are manifested in a violation of time translation invariance of the two times correlation functions [14] analogous to those of glass formers or granular media [24, 28, 29].

These simulations also reproduce the experimentally found time dependence of the critical current [13]. Usually, one defines an effective critical current, $I_{\rm c}^{\rm eff}$, as the point where V becomes larger than a given threshold (say $V_{\rm thr} = 5 \times 10^{-5}$ in our case): one then finds that $I_{\rm c}^{\rm eff}$ is t_0 and I_0 dependent. For instance, like in experiments [13] $I_{\rm c}^{\rm eff}$ is slowly increasing with t_0 (see figure 18: at $T = 0.1$ and $N_{\rm ext} = 10$ for a drive $I_0 = 1$); we find that $I_{\rm c}^{\rm eff}$ increases approximately logarithmically with t_0:

$$I_{\rm c}^{\rm eff}(t_0) \simeq J_1 + J_2 \ln(t_0) \tag{9}$$

with $J_1 \simeq 0.15$, $J_2 \simeq 0.008$ (the dotted line of figure 18).

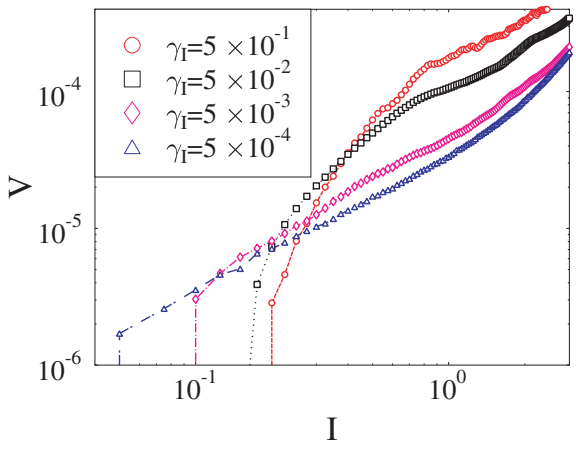

Figure 19. The I–V is measured at $T = 0.1$ and $N_{\rm ext} = 0.4$ in a sample with very strong pinning sites, $A_0^p = 10A_0$, and small pinning density, $p = 0.2$. We show here the non-linear behaviour of the I–V and their dependence on γ_I, signalling the off-equilibrium status of the system.

The existence of the slow part in the $V(t)$ relaxation also affects the 'stiffening' of the response in the I–V of figure 17, which is due to the non-stationarity of the vortex flow on scales smaller than τ_V. Actually, in figure 17, for a given I the value of V on the different curves corresponds to the system being probed at different stages of its non-stationary evolution (this also outlines that the proper definition of $I_{\rm c}$ is the *asymptotic* one).

4.4. Role of pinning

Finally, an important question arising in the context of vortex physics concerns the effects that pinning has on transport properties. We discuss such a topic in the present section where we consider higher pinning strength, A_0^p, and different fractions on pinning sites, p. In particular, we study the strong pinning case where $A_0^p = 10A_0$ (to compare to the cases $A_0^p = 0.3$ previously discussed). The general picture depicted up to here in the paper is not altered, however some interesting features appear.

The I–V curves (analogous to those reported in figure 12 where $A_0^p = 0.3$), at $T = 0.1$ and $N_{\rm ext} = 0.4$, are shown in figure 19 in the case of strong pinning strength $A_0^p = 10A_0$ and small pinning fraction $p = 0.2$. The apparent dependence of the I–V function on the current ramp rate is also clearly observable here. The basic difference with the weak pinning case dealt with before is that now a definite *finite* threshold current, $I_{\rm c}^{\rm eff}$, appears above which the voltage is positive. Importantly, the value of such a threshold is still dependent on the current ramp rate γ_I, as shown in figure 20. The points $I_{\rm c}^{\rm eff}(\gamma_I)$ can be reasonably well interpolated by a power law:

$$I_{\rm c}^{\rm eff}(\gamma_I) \simeq J_r \gamma_I^{x_p} + J_0 \tag{10}$$

where $J_r \simeq 0.25$, $J_0 \simeq 0.0$ and the exponent $x_p \simeq 0.2$. Since the exponent x_p is small a log fit could work too, but more interesting is the fact that J_0 is numerically zero. This implies that in the present case with strong pinning strength and small pinning density, the 'equilibrium' critical current, J_0, is indeed zero. This is consistent with the presence of a zero $T_{\rm c}$ and with the fact that we are at a finite T. These findings too are in strict analogy to recent experimental observations [13].

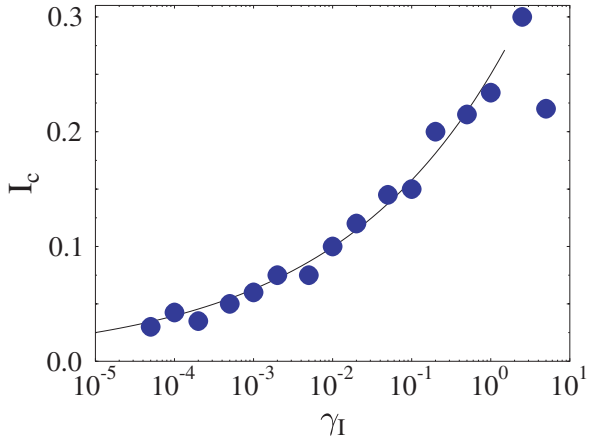

Figure 20. For the data of figure 19, we define the critical current, I_c, as the point where $V > 0$ (within our numerical accuracy $\Delta V = 10^{-6}$). Interestingly, in agreement with recent experimental data, $I_c(\gamma_I)$ seems to increase with γ_I. The superimposed curve is the fit discussed in the text.

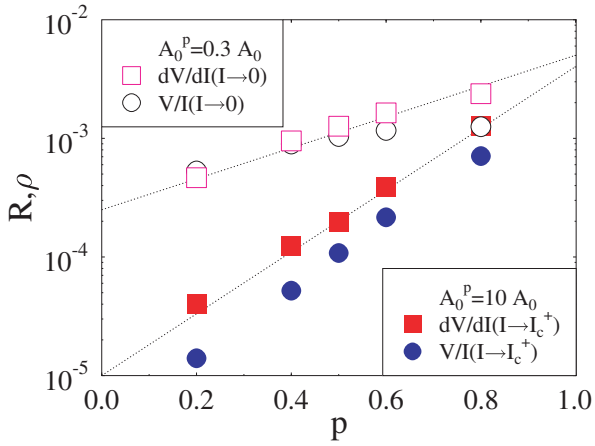

Figure 21. The dependence of resistivity, $R = V/I$, and differential resistivity, $\rho = \mathrm{d}V/\mathrm{d}I$, on the pinning density, p, and strength, A_0^p, are plotted here at $T = 0.1$ and $N_{\mathrm{ext}} = 0.4$ (for $\gamma_I = 5 \times 10^{-4}$).

Finally (see figure 21), we have studied the resistivity, R, and the differential resistivity, ρ, as a function of the fraction of pinning sites, p, in the system for two values of their strength A_0^p. Figure 21 shows that R and ρ strongly increase with p, but they decrease with A_0^p.

4.5. Summary

Summarizing, in this section we have seen that for low T the I–V characteristics in the ROM model have the typical *non-linear*, S shape form experimentally found. They have approximately *power law* behaviours which are dependent on the current ramp rate γ_I. For weak pinning strength, *Ohmic* behaviour is recovered when $\gamma_I \to 0$. Whenever $\gamma_I > \tau_V^{-1}$, the function $V(I)$ depends on the system history, simply because the system has not been able to follow the drive. Of practical relevance is the finding that for large γ_I the effective

resistivity measured in the sample is larger than the intrinsic one (i.e. the one derived from the 'asymptotic I–V'). We also showed that for I–V recorded far from stationarity an approximate *scaling structure* à la Fisher is found, whose precise nature is still to be understood. We have also outlined the presence of a clear *peak effect* (PE) in critical currents. The location of the maximum in the PE as a function of the external field is importantly very close to the values of the *second magnetization peak* found in magnetic loops; their values coincide for $\gamma_I \to 0$ [39]. We have also discussed *'memory'* phenomena observed in I–Vs, such as its interesting *stiffening* behaviours. We stress that known experimental facts on vortex matter are in agreement with all the above listed properties of the present model.

5. Conclusions

We have demonstrated that a comprehensive phenomenology, consistent with known experiments, of transport properties of vortex matter can be derived from a simple Monte Carlo driven lattice model of the vortex system. In this schematic model vortices are dealt with as 'particles', interacting among themselves and with a pinning random background. They undergo a diffusion thermal dynamics under an external drive.

Our results are briefly summarized in sections 3.2 and 4.5. In a few words, we found that important 'history' dependent phenomena observed at low temperatures (as in the PE region) originate from the properties of the system characteristic timescales, $\tau_V(T, N_{\rm ext}, I)$, which diverge a low T and has a broad maximum as a function of the external field around the PE. In particular, the PE, observed in transport properties as a function of the applied field, corresponds to a first order phase transition found in the un-driven system at equilibrium, which in turn is manifested as a second peak in magnetic hysteresis loops [39]. We have also discussed important properties of I–V, critical current and resistivity. All these phenomena can be addressed within the general scenario of off-equilibrium 'glassy' dynamics of the ROM model.

We have restricted our investigation here to a system of rigid parallel vortices, corresponding to a two dimensional version of our model. The main effect of the restriction to two dimensions is that the thermodynamic glass transition temperature $T_{\rm c}$ is zero, whereas in higher dimensions $T_{\rm c}$ may be non-zero. For the present general discussion about off-equilibrium phenomena this fact is, however, not crucial, since phenomenological behaviours found above the transition temperature (manifested through logarithmically slow time dependence of creep, 'memory and hysteretic' effects in I–V, etc) are very similar in the two cases. The significant slowing down at low temperatures makes it difficult in experiments, as well as in simulations, to approach equilibrium in the vicinity of $T_{\rm c}$: this is only possible at temperatures above the phenomenological glass transition temperature $T_{\rm g}$—the temperature where the characteristic timescale of the system becomes much longer than any affordable experimental or simulation timescale. The off-equilibrium physics around $T_{\rm g}$ looks much the same whether $T_{\rm c}$ is zero or non-zero.

The present model appears to describe a broad range of phenomena found in vortex matter, including a variety of magnetic and transport properties. In this respect, its simple physical mechanisms may indeed catch some important aspect of vortex physics [1–4], as the application of driven lattice gases theory [15] to off-equilibrium properties of vortex matter may open further interesting developments.

Acknowledgments

This work was supported by EPSRC, Progetto Scambi Internazionali Universitá di Napoli 'Federico II', ESF Sphinx Program, MURST-PRIN 2002, MIUR-FIRB 2002, CRdC-AMRA, INFM-PCI.

References

[1] Blatter G, Feigel'man M V, Geshkenbein V B, Larkin A I and Vinokur V M 1994 *Rev. Mod. Phys.* **66** 1125
[2] Brandt E H 1995 *Rep. Prog. Phys.* **58** 1465
[3] Yeshurun Y, Malozemoff A P and Shaulov A 1996 *Rev. Mod. Phys.* **68** 911
[4] Cohen L F and Jensen H J 1997 *Rep. Prog. Phys.* **60** 1581
[5] Larkin A I and Ovchinnikov Yu N 1979 *J. Low Temp. Phys.* **34** 409
[6] Le Doussal P and Gianmarchi T 1998 *Phys. Rev.* B **57** 11356
[7] Jensen H J, Brass A and Berlinsky A J 1988 *Phys. Rev. Lett.* **60** 1676
[8] Nori F 1996 *Science* **276** 1373
[9] Olson C J, Reichhardt C and Nori F 1998 *Phys. Rev. Lett.* **81** 3757
[10] Kolton A B, Dominguez D and Gronbech-Jensen N 1999 *Phys. Rev. Lett.* **83** 3061
[11] Reichhardt C, van Otterlo A and Zimanyi G T 2000 *Phys. Rev. Lett.* **84** 1994
[12] Bhattacharya S and Higgins M J 1993 *Phys. Rev. Lett.* **70** 2617
Bhattacharya S and Higgins M J 1995 *Phys. Rev.* B **52** 64
Henderson W, Andrei E Y, Higgins M J and Bhattacharya S 1996 *Phys. Rev. Lett.* **77** 2077
[13] Xiao Z L, Andrei E Y and Higgins M J 1999 *Phys. Rev. Lett.* **83** 1664
Xiao Z L, Andrei E Y, Shuk P and Greenblatt M 2000 *Phys. Rev. Lett.* **85** 3265
[14] Nicodemi M and Jensen H J 2001 *Phys. Rev. Lett.* **86** 4378
Nicodemi M and Jensen H J 2001 *Phys. Rev. Lett.* **87** 259702
Nicodemi M and Jensen H J 2002 *Phys. Rev.* B **65** 144517
Nicodemi M and Jensen H J 2001 *J. Phys. A: Math. Gen.* **34** L11
Nicodemi M and Jensen H J 2001 *J. Phys. A: Math. Gen.* **34** 8425
Nicodemi M and Jensen H J 2001 *Europhys. Lett.* **54** 566
Nicodemi M and Jensen H J 2002 *Europhys. Lett.* **57** 348
[15] Katz S, Lebowitz J L and Spohn H 1983 *Phys. Rev.* B **28** 1655
Schmittmann B and Zia R K P 1995 *Phase Transition and Critical Phenomena* vol 17, ed C Domb and J L Lebowitz (London: Academic)
Marro J and Dickman R 1999 *Nonequilibrium Phase Transitions in Lattice Models* (Cambridge: Cambridge University Press)
[16] Binder K 1997 *Rep. Prog. Phys.* **60** 487
[17] Wordenweber R, Kes P H and Tsuei C C 1986 *Phys. Rev.* B **33** 3172
[18] Kwok W K *et al* 1994 *Phys. Rev. Lett.* **72** 1092
[19] Safar H *et al* 1995 *Phys. Rev.* B **52** 6211
[20] Wen H H, Li S L, Chen G H and Ling X L 2001 *Phys. Rev.* B **64** 054507
[21] Campion R P, King P J, Benedict K A, Bowley R M, Czerwinka P S, Misat S and Morley S M 2000 *Phys. Rev.* B **61** 6387
[22] Paltiel Y *et al* 2000 *Nature* **403** 398
[23] Götze W and Sjögren L 1992 *Rep. Prog. Phys.* **55** 241
[24] Angell C A 1995 *Science* **267** 1924
Ediger M D, Angell C A and Nagel S R 1996 *J. Phys. Chem.* **100** 13200
Bouchaud J P, Cugliandolo L F, Kurchan J and Mezard M 1997 *Spin Glasses and Random Fields* ed A P Young (Singapore: World Scientific)
[25] Lefloch F, Hamman J, Ocio M and Vincent E 1992 *Europhys. Lett.* **18** 647
Jonason K, Vincent E, Hamman J, Bouchaud J P and Nordblad P 1998 *Phys. Rev. Lett.* **81** 3243
[26] Bassler K E and Paczuski M 1998 *Phys. Rev. Lett.* **81** 3761
Bassler K E, Paczuski M and Altshuler E 2001 *Phys. Rev.* B **64** 224517
[27] Monier D and Fructer L 2000 *Eur. Phys. J.* B **17** 201
[28] Caiazzo A, Coniglio A and Nicodemi M 2002 *Phys. Rev.* E **66** 046101
Caiazzo A, Coniglio A and Nicodemi M 2004 *Europhys. Lett.* **65** 256
Coniglio A, de Candia A, Fierro A and Nicodemi M 1999 *J. Phys.: Condens. Matter* **11** A167
[29] Nicodemi M, Coniglio A and Herrmann H J 1997 *Phys. Rev.* E **55** 3962
Coniglio A and Nicodemi M 2000 *J. Phys.: Condens. Matter* **12** 6601
Nicodemi M 2000 *Physica* A **285** 267
Nicodemi M 1998 *Physica* A **257** 448
Nicodemi M 1999 *Phys. Rev. Lett.* **82** 3734
Tarzia M, de Candia A, Fierro A, Nicodemi M and Coniglio A 2004 *Europhys. Lett.* **66** 531
[30] Hyman R A, Wallin M, Fisher M P A, Girvin S M and Young A P 1995 *Phys. Rev.* B **51** 15304

[31] D'Anna G *et al* 1995 *Phys. Rev. Lett.* **75** 3521
[32] This is confirmed in MD simulations by Reichhardt C *et al* 1995 *Phys. Rev.* B **52** 10441
Reichhardt C *et al* 1996 *Phys. Rev.* B **53** R8898
[33] Giller D, Shaulov A, Tamegai T and Yeshurun Y 2000 *Phys. Rev. Lett.* **84** 3698
van der Beek C J, Colson S, Indenbom M V and Konczykowski M 2000 *Phys. Rev. Lett.* **84** 4196
[34] Wen H-H *et al* 1998 *Phys. Rev. Lett.* **80** 3859
[35] Koshelev A E and Vinokur V M 1994 *Phys. Rev. Lett.* **73** 3580
Balents L and Fisher M P A 1995 *Phys. Rev. Lett.* **75** 4270
Giamarchi T and Le Doussal P 1996 *Phys. Rev. Lett.* **76** 3408
[36] Fisher M P A 1989 *Phys. Rev. Lett.* **62** 1415
Fisher D S, Fisher M P A and Huse D A 1991 *Phys. Rev.* B **43** 130
[37] Koch R H, Foglietti V, Gallager W J, Koren G, Gupta A and Fisher M P A 1989 *Phys. Rev. Lett.* **63** 1511
[38] Olsson P and Teitel S 2001 *Phys. Rev. Lett.* **87** 137001
Vestergren A, Lidmar J and Wallin M 2002 *Phys. Rev. Lett.* **88** 117004
[39] Nicodemi M 2002 *J. Phys.: Condens. Matter* **14** 2403
Nicodemi M 2003 *Fractals* **11** 149
Nicodemi M 2003 *Phys. Rev.* E **67** 041103
[40] Pippard A B 1969 *Phil. Mag.* **19** 217
[41] Bhattacharya S and Higgins M J 1994 *Phys. Rev.* B **49** 10005
Higgins M J and Bhattacharya S 1996 *Physica* C **257** 232 and references therein
Sarkar S *et al* 2000 *Phys. Rev.* B **61** 12394
[42] De Sorbo W 1964 *Rev. Mod. Phys.* **36** 90
Kes P H and Tsuei C C 1983 *Phys. Rev.* B **28** 5126
Tamegai T *et al* 1993 *Physica* C **213** 33
Yang G *et al* 1993 *Phys. Rev.* B **48** 4054
Yeshurun Y *et al* 1994 *Phys. Rev.* B **49** 1548
Zeldov E *et al* 1995 *Nature* **375** 373
Khaykovich B *et al* 1996 *Phys. Rev. Lett.* **76** 2555
Khaykovich B *et al* 1997 *Phys. Rev.* B **56** R517
Gammel P L *et al* 1998 *Phys. Rev. Lett.* **80** 833
Shi J *et al* 1999 *Phys. Rev.* B **60** 12593
Radzyer Y *et al* 2000 *Phys. Rev.* B **61** 14362
[43] Banerjee S S *et al* 1998 *Phys. Rev.* B **58** 995
Ravikumar G *et al* 2000 *Phys. Rev.* B **61** 12490
Banerjee S S *et al* 2001 *Physica* C **355** 39
[44] Glazman L I and Koshelev A E 1991 *Phys. Rev.* B **43** 2835
Daemen L L *et al* 1993 *Phys. Rev. Lett.* **70** 1167
Koshelev A E and Kes P H 1993 *Phys. Rev.* B **48** 6539
Krusin-Elbaum L *et al* 1992 *Phys. Rev. Lett.* **69** 2280
Larkin A I *et al* 1995 *Phys. Rev. Lett.* **75** 2992
Tang C *et al* 1996 *Europhys. Lett.* **35** 597
[45] Giamarchi T and Le Doussal P 1997 *Phys. Rev.* B **55** 6577
[46] van Otterloo A *et al* 2000 *Phys. Rev. Lett.* **84** 2493
[47] Cubitt R *et al* 1993 *Nature* **365** 407
Lee S L *et al* 1993 *Phys. Rev. Lett.* **71** 3862
Kwok W K *et al* 1994 *Phys. Rev. Lett.* **73** 2614
Galifullin M B *et al* 2000 *Phys. Rev. Lett.* **84** 2945
Sonier J E *et al* 2000 *Phys. Rev.* B **61** R890
[48] Kokkaliaris S *et al* 1999 *Phys. Rev. Lett.* **82** 5116
Kokkaliaris S *et al* 1999 *J. Low Temp. Phys.* **117** 1341
Rassau A P *et al* 2000 *Physica* B **284–288** 693
Konczykowski M *et al* 2000 *Physica* C **332** 219
Giller D *et al* 1997 *Phys. Rev. Lett.* **79** 2542
[49] Correa V F, Nieva G and de la Cruz F 2001 *Phys. Rev. Lett.* **87** 057003
[50] Tang C, Ling X, Bhattacharya S and Chaikin P M 1996 *Europhys. Lett.* **35** 597